HHS Public Access

Author manuscript

Nanotoxicology. Author manuscript; available in PMC 2018 May 24.

Published in final edited form as:

Nanotoxicology. 2017 February ; 11(1): 41–51. doi:10.1080/17435390.2016.1262919.

TIMP1 promotes multi-walled carbon nanotube-induced lung fibrosis by stimulating fibroblast activation and proliferation

Jie Dong and **Qiang Ma**

Receptor Biology Laboratory, Toxicology and Molecular Biology Branch, Health Effects Laboratory Division, National Institute for Occupational Safety and Health, Centers for Disease Control and Prevention, Morgantown, WV, USA

Abstract

Pulmonary exposure to multi-walled carbon nanotubes (MWCNTs) may cause fibrosing lesions in animal lungs, raising health concerns about such exposure in humans. The mechanisms underlying fibrosis development remain unclear, but they are believed to involve the dysfunction of fibroblasts and myofibroblasts. Using a mouse model of MWCNT exposure, we found that the tissue inhibitor of metalloproteinase 1 (Timp1) gene was rapidly and highly induced in the lungs by MWCNTs in a time- and dose-dependent manner. Concomitantly, a pronounced elevation of secreted TIMP1 was observed in the bronchoalveolar lavage (BAL) fluid and serum. Knockout (KO) of Timp1 in mice caused a significant reduction in fibrotic focus formation, collagen fiber deposition, recruitment of fibroblasts and differentiation of fibroblasts into myofibroblasts in the lungs, indicating that TIMP1 plays a critical role in the pulmonary fibrotic response to MWCNTs. At the molecular level, MWCNT exposure significantly increased the expression of the cell proliferation markers Ki-67 and PCNA and a panel of cell cycle-controlling genes in the lungs in a TIMP1-dependent manner. MWCNT-stimulated cell proliferation was most prominent in fibroblasts but not myofibroblasts. Furthermore, MWCNTs elicited a significant induction of CD63 and integrin β1 in lung fibroblasts, leading to the formation of a TIMP1/CD63/integrin β1 complex on the surface of fibroblasts *in vivo* and *in vitro*, which triggered the phosphorylation and activation of Erk1/2. Our study uncovers a new pathway through which induced TIMP1 critically modulates the pulmonary fibrotic response to MWCNTs by promoting fibroblast activation and proliferation via the TIMP1/CD63/integrin β1 axis and ERK signaling.

Keywords

TIMP1; multi-walled carbon nanotube; lung fibrosis; fibroblast; myofibroblast

CONTACT Qiang Ma qam1@cdc.gov.

Supplemental data for this article can be accessed here.

Declaration of interest

The authors declare there are no competing financial interests.

Introduction

Carbon nanotubes (CNTs) are new nanomaterials with potentials for a broad range of applications (De Volder et al., 2013). There has been a rapid increase in the development and production of CNT-based materials in recent years. However, the increased production and utility of CNT materials may lead to greater human exposure to CNTs. The physicochemical properties of CNTs, such as their nanoscale size, fiber-like shape and high biopersistence and respirability, have led to concern over the possible adverse effects of CNTs on human health (Donaldson et al., 2010; Dong & Ma, 2015; Johnston et al., 2010).

A major finding from studies on CNT health effects is that pulmonary exposure to certain forms of CNTs causes fibrosing lesions in the lungs of exposed animals (Aiso et al., 2010; Dong et al., 2015; Porter et al., 2010; Reddy et al., 2012). In these scenarios, lung fibrosis induced by CNTs resembles the pulmonary response to deposition of fibrogenic foreign bodies, manifesting an early phase response that features rapid-onset fibrosis alongside acute inflammatory infiltration and cytokine expression, followed by resolution of the acute pathology and progression to chronic interstitial fibrosis and granuloma formation. Notably, CNT-induced lung fibrosis displays a high degree of similarity to silica- or asbestos-induced pneumoconiosis and to idiopathic pulmonary fibrosis (IPF), both of which are poorly understood, progressive and incurable human fibrosing lung diseases, raising the possibility that exposure to CNTs potentially leads to lung fibrotic lesions or diseases in humans.

Pathologically, fibrosis is characterized by the excessive production and deposition of extracellular matrix (ECM) components in injured tissue to lead to scarring and tissue destruction. The underlying mechanisms are poorly understood, but they are believed to involve the dysregulation and dysfunction of fibroblasts and myofibroblasts, major effector cells that mediate matrix production, remodeling and contraction in fibrosis development (Wynn & Ramalingam, 2012). Under physiologic conditions, the lung resident fibroblasts in the interstitial space are largely “quiescent,” but they are required for the maintenance of normal matrix homeostasis. Upon tissue injury, fibroblasts are activated, and activated fibroblasts migrate to the injured sites, proliferate and differentiate into myofibroblasts. Myofibroblasts are characterized by their *de novo* synthesis of α-smooth muscle actin (α-SMA), which is incorporated into stress fibers to mediate matrix contraction and scar formation (Dong & Ma, 2016b; Hinz, 2010; Tomasek et al., 2002). Myofibroblasts also possess a high capacity of protein synthesis and secretion and are, therefore, believed to be responsible for the production of a major proportion of fibrotic matrix proteins within fibrotic foci. The majority of myofibroblasts undergo apoptosis upon physiologic wound healing. On the other hand, these cells persist and remain active during pathologic fibrosis. The molecular mechanisms controlling the dynamics and behaviors of fibroblasts and myofibroblasts during lung fibrosis are largely unknown, which is in part due to a lack of appropriate animal models of lung fibrosis to mimic human pulmonary fibrosing diseases, and to a lack of molecular insights into the pathways that dictate fibroblast recruitment, proliferation, differentiation and turnover during lung fibrosis.

The tissue inhibitor of metalloproteinase 1 (TIMP1) is a glycoprotein of the TIMP family (Stetler-Stevenson, 2008). TIMP1 is secreted into the ECM by activated macrophages and

other cells to inhibit matrix metalloproteinases (MMPs) and thereby plays a role in matrix remodeling. Recent evidence reveals that secreted TIMP1 may function as a paracrine and/or autocrine factor to promote cell proliferation and inhibit apoptosis through the CD63/integrin β1-dependent activation of intracellular pathways, such as ERK signaling. Moreover, TIMP1 is secreted into the plasma in certain fibrosing diseases and cancers and, therefore, affects distant tissues in a manner analogous to an endocrine factor. Consistent with this notion, TIMP1 is highly induced during fibrosis in a number of animal models, such as bleomycin- and paraquat-induced lung fibrosis, and fibrosing diseases in humans, such as IPF and liver cirrhosis, implicating dysregulation of TIMP1 expression in the development of fibrosis (Dong et al., 2016; Hayashi et al., 1996; Madtes et al., 2001; Manoury et al., 2006; Selman et al., 2000; Tomita et al., 2007). Nonetheless, the function of TIMP1 in fibrosis, in particular, in the development of lung fibrosis remains largely unclear.

In light of the presumed multiple roles of TIMP1 in tissue fibrosis, we attempted to characterize Timp1 expression and analyze its role, if any, during multi-walled carbon nanotube (MWCNT)-induced lung fibrosis. Our findings revealed that Timp1 was rapidly and highly induced by MWCNTs at both the mRNA and protein levels in a time- and dose-dependent manner in mouse lungs. Induced TIMP1 was secreted and accumulated in the bronchoalveolar lavage (BAL) and serum to high levels, suggesting TIMP1 as a highly inducible protein marker for detecting and monitoring MWCNT lung exposure and health effects. By utilizing Timp1 knockout (KO) mice, we showed that TIMP1 is a pro-fibrotic factor toward CNT-induced lung fibrosis and identified a TIMP1-mediated mechanism that potentially underlies the fibrotic response to CNT exposure in the lungs.

Materials and methods

Multi-walled carbon nanotubes

MWCNTs were obtained from Mitsui & Company (XNRI MWNT-7, lot #05072001K28, Tokyo, Japan) and have been characterized previously (Dong et al., 2015; Porter et al., 2010). The MWCNTs have an average surface area of 26 m^2/g as measured by nitrogen absorption–desorption technique (Brunauer–Emmett–Teller method, or BET); and a median length of 3.86 μm and count mean diameter of 49 ± 13.4 nm, as determined by scanning electron microscopy when suspended in a dispersion medium (DM). Trace element contaminations are low, with 0.78% for all metals, 0.41% for sodium and 0.32% for iron.

DM was used to disperse MWCNTs and was used as the vehicle control, containing 0.6 mg/ml mouse serum albumin (Sigma-Aldrich, St. Louis, MO) and 0.01 mg/ml 1,2-dipalmitoyl-sn-glycerol-3-phosphocholine (Sigma-Aldrich) in Ca^{2+}- and Mg^{2+}-free PBS, pH7.4. DM was freshly prepared before use. MWCNTs were dispersed in DM with a two-step sonication immediately before use. DM effectively disperses MWCNTs as shown by transmission electron microscopy in which the width distribution of MWCNTs followed a normal distribution and the length distribution was log normal (Porter et al., 2010). The DM preparation does not cause toxicity or mask the reactivity of MWCNTs at the dose range used in this study (Dong & Ma, 2016c).

Animals and treatment

Eight- to 10-week-old male C57BL/6J (WT) and B6.129S4-Timp1tm1Pds/J (Timp1 KO) mice were purchased from The Jackson Laboratory (Bar Harbor, ME). The mice were maintained in an accredited, specific pathogen-free and environmentally controlled facility at the National Institute for Occupational Safety and Health. All experiments involving animals were approved by the Institutional Animal Care and Use Committee. A single dose of 50 μl of DM or MWCNT suspension was administered by pharyngeal aspiration as described previously (Porter et al., 2010).

Histopathology

The mice were euthanized and the left lung lobe was fixed with 10% neutral buffered formalin and embedded in paraffin. Sections of 5 μm thickness were used to perform Masson's Trichrome staining and Picro-Sirius Red staining following standard protocols. Six samples per group were observed and evaluated.

Immunohistochemistry and immunofluorescence

Formalin-fixed, paraffin-embedded lung tissue sections were deparaffinized, antigen-unmasked and used to perform immunohistochemistry; and cryostat sections from frozen lung tissues were fixed with 4% paraformaldehyde and used for immunofluorescence. Both methods were described in detail in Supplemental materials and in a previous report (Dong & Ma, 2016a).

Primary mouse lung fibroblast culture, *in vitro* cell proliferation and inhibition, PCR array, quantitative RT-PCR, microarray analyses, enzyme-linked immunosorbent assay, and immunoblotting and quantification

These assays were performed according to standard procedures and were described in detail in Supplemental materials.

Statistical analysis

The statistical evaluation of differences between experimental groups was performed using one-way ANOVA followed by between group comparisons using standard procedures. Major quantitative experiments were repeated at least once, and representative data were presented as the mean ± standard deviation (SD). A p value of less than 0.05 was considered statistically significant. *$p < 0.05$; **$p < 0.01$; and ***$p < 0.001$.

Results

Rapid and pronounced induction and secretion of TIMP1 in mouse lungs exposed to MWCNTs

Preliminary experiments revealed that exposure to MWCNTs induces lung Timp1 expression and the induction is most prominent within 14 d post-exposure, which correlates with the early phase response to MWCNT exposure in mouse lungs (Dong et al., 2015). Therefore, all subsequent studies focused on Timp1 expression during the early phase response to MWCNTs.

Adult C57BL/6J mice were treated with DM (the vehicle control) or MWCNTs at 40 μg per mouse by pharyngeal aspiration. The lungs were harvested on days 1, 3, 7 and 14 after treatment. We first performed a PCR array analysis. Expression of Timp1 was low in DM-treated lungs, indicating the low expression of Timp1 in the lungs under basal conditions. Upon exposure to MWCNTs, Timp1 mRNA expression was markedly increased with a peak at 1 d post-exposure (a 24-fold increase, Figure 1A). Induction of Timp1 was verified by quantitative RT-PCR (qRT-PCR) using RNA samples from individual mice, confirming the induction of Timp1 with maximal induction occurring at 1 d (a 13-fold increase), followed by reduced, but significantly elevated over the control, expression from 3 to 14 d (Figure 1B).

The basal expression of TIMP1 protein was low in the DM-exposed lungs, but the level of TIMP1 was significantly elevated by MWCNTs, in agreement with the mRNA expression results (Figure 1C). One day post-exposure, accumulation of induced TIMP1 was observed in the alveolar septa throughout the lungs, whereas on days 3, 7 and 14 after exposure, accumulation of TIMP1 was most apparent within the interstitial fibrotic foci where MWCNTs deposited (Figure 1C).

TIMP1 protein was detected by enzyme-linked immunosorbent assay (ELISA) at low levels in the BAL from DM-treated mice, but the amount was strikingly elevated by MWCNTs, to extremely high levels after 1 d (from 36.0 to 5287.8 pg/ml) and 3 d (from 12.4 to 7187.6 pg/ml) and to reduced, but statistically significant, levels after 7 d (from 16.9 to 367.2 pg/ml) and 14 d (from 29.5 to 94.2 pg/ml) (Figure 1D, left panel). The level of TIMP1 protein in the serum was also significantly increased at all-time points examined, even though the basal level of serum TIMP1 was high compared with those in the BAL and lung tissues (Figure 1D, right panel). The peak level was observed at 1 d (from 420.8 to 1630.8 pg/ml) and induction slowly declined from 3 to 14 d.

MWCNTs at a single dose of 5 μg per mouse (7 d) caused a significant increase of the TIMP1 level in the BAL fluid (Figure 1E, left panel) but not in the serum (Figure 1E, right panel), which may reflect a higher basal level of TIMP1 in the serum than in the BAL. Treatment with 20 or 40 μg of MWCNTs led to significant increases of TIMP1 levels in both the BAL fluid and serum, with a more dramatic induction in the BAL fluid than in the serum (Figure 1E). Thus, MWCNTs potently induced TIMP1 secretion into the BAL and serum dose-dependently, which correlates with induction of fibrosis by MWCNTs (Dong et al., 2015).

TIMP1 is synthesized and secreted into the extracellular space by a number of types of cells, such as macrophages, fibroblasts and lung epithelial cells, in an inducer-, time- and context-dependent manner. To identify major sources of TIMP1 induced by MWCNTs, we compared TIMP1 induction in macrophages, fibroblasts and epithelial cells in the alveolar region by immunofluorescence co-staining of TIMP1 with Mac2 (galectin 3), Hsp47 (heat shock protein 47) and E-cadherin, which are known marker proteins for macrophages, fibroblasts and epithelial cells, respectively. Under a basal condition, Hsp47+ fibroblasts and E-cadherin+ alveolar epithelial cells were major cell types in the region, whereas Mac2+ macrophages were detected sparsely (Figure S1, upper panel). Upon exposure, Hsp47+

fibroblasts became predominate cells in fibrotic regions, followed by E-cadherin+ epithelial cells and lastly Mac2+ macrophages (Figure S1, lower panel). Notably, most, if not all, Hsp47+ fibroblasts and Mac2+ macrophages co-stained with TIMP1, whereas most E-cadherin+ cells were negative for TIMP1 staining. Moreover, TIMP1 was detected both on the cell surface and in the cytoplasm of fibroblasts and macrophages, suggesting that TIMP1 is in part derived from these cells. We further demonstrated the induction of TIMP1 by MWCNTs in cultured primary mouse lung fibroblasts, which confirms the *de novo* synthesis of TIMP1 in fibroblasts (Figure S2). Therefore, Hsp47+ fibroblasts are a predominant source of TIMP1 production, followed by Mac2+ macrophages, within the fibrotic foci of the lungs exposed to MWCNTs for 7 d.

Reduced fibrotic response to MWCNTs in Timp1 KO lungs

To analyze the function of Timp1, we compared the fibrotic phenotype of Timp1 KO (Timp1−/−) lungs with WT. The induction of fibrotic changes by MWCNTs was observed in both WT and Timp1 KO lungs, but to a much lower degree in Timp1 KO lungs, as assessed by the number and size of fibrotic foci at all-time points examined (Figures 2A and S3). The fibrotic response reached a peak level at 7 d post-exposure in both WT and Timp1 KO lungs; however, there was a remarkably lower amount of collagen fibers deposited in the fibrotic foci of Timp1 KO lungs than in those of WT lungs, as determined by both Masson's Trichrome staining and Picro-Sirius Red staining (Figure S4).

MWCNTs increased the deposition of Collagen I and fibronectin (FN1), two major matrix proteins in lung fibrosis, in fibrotic areas in both WT and Timp1 KO lungs; however, there were significantly lower levels of both proteins in Timp1 KO than WT lungs at 7 d post-exposure, as shown by immunofluorescence (Figure 2B) and immunohistochemistry (Figure S5). Immunoblotting further confirmed the induction of FN1 in the lungs by MWCNTs and reduced levels of FN1 induction in Timp1 KO than WT lungs in a time-dependent manner (Figures 2C and S6).

The development of pulmonary fibrosis depends on the activation and recruitment of fibroblasts and their differentiation into myofibroblasts. To examine these cells, we chose Vimentin and FSP1 (fibroblast specific protein 1) in addition to Hsp47 as markers for fibroblasts, and α-SMA and PDGFR-β (platelet-derived growth factor receptor, β polypeptide) as markers for myofibroblasts. Positive staining for both Hsp47 (Figure 3A, upper panel) and Vimentin (Figure 3A, lower panel) was markedly elevated in the fibrotic foci of MWCNT-exposed lungs, but the degree of increase was significantly lower in Timp1 KO than WT lungs, especially in the case of Vimentin. Immunoblotting showed induction of FSP1 by MWCNTs in the lungs, but induction in Timp1 KO lungs was markedly lower than that in WT, especially on days 3 and 14 post-exposure (Figures 3B and S7).

Immunofluorescence staining revealed that α-SMA+ or PDGFR− β+ myofibroblasts were dramatically increased by MWCNTs in the fibrotic foci of WT lungs but only slightly induced in the fibrotic foci of Timp1 KO lungs (Figure 3C). The difference between MWCNT-treated WT and Timp1 KO lungs was statistically significant for both α-SMA and PDGFR-β. Immunohistochemistry staining confirmed markedly increased α-SMA+ myofibroblasts in fibrotic regions induced by MWCNTs and the increase was more

significant in WT than Timp1 KO lungs (Figure 3D), which was consistently observed at all-time points tested (Figure S8). Therefore, although exposure to MWCNTs markedly increases the numbers of fibroblasts and myofibroblasts in fibrosing regions, loss of TIMP1 significantly reduces the magnitude of the increase compared with WT.

Stimulation of cell proliferation in mouse lungs by MWCNTs and TIMP1

We tested whether increased cellularity reflects increased cell proliferation during fibrosis development by detecting the expression of Ki-67 (marker of proliferation Ki-67) and PCNA (proliferating cell nuclear antigen), two commonly used markers for proliferating cells. Immunohistochemistry clearly showed that Ki-67+ cells (Figures 4A and S9; upper panels) and PCNA+ cells (Figures 4A and S9; lower panels) were dramatically increased in fibrotic foci in MWCNT-treated lungs compared with the control during the early phase response to MWCNTs, with a peak level at 7 d. Immunoblotting of whole protein extracts from lung tissues showed an apparent induction of PCNA expression by MWCNTs at 3 and 7 d post-exposure, and a slight induction at 1 and 14 d (Figures 4B and S10).

We examined whether TIMP1 modulates fibrosis by affecting MWCNT-induced cell proliferation. Immunofluorescence staining of Ki-67 (Figure 4C, upper panel) or PCNA (Figure 4C, lower panel) showed that the numbers of Ki-67+ or PCNA+ cells were significantly increased in the fibrotic foci of both WT and Timp1 KO lungs exposed to MWCNTs; however, the increase was markedly less apparent in Timp1 KO than WT lungs. Immunoblotting showed that the PCNA level was induced by MWCNTs in both WT and Timp1 KO lungs, but the induction was apparently lower in Timp1 KO than WT lungs at 1, 3 and 7 d (Figures 4D and S11). Thus, TIMP1 is required for a maximal cell proliferation response to MWCNTs in mouse lungs.

We performed a genome-wide gene expression analysis on RNA samples isolated from WT or Timp1 KO lungs exposed to DM or 40 μg of MWCNTs for 7 d. Four randomly selected samples were studied for each genotype and treatment group. We identified 21 genes involved in cell cycle control that exhibited significant induction by MWCNTs in WT but not Timp1 KO lungs. Heat map analysis of these differentially expressed genes is presented in Figure 5(A), and detailed expression levels and data analysis are listed in Table S1. The fold changes and statistical analyses among genotypes and treatment groups for eight of these genes, including Bub1b, Capg, Cenpa, Kif2c, Kif22, Mcm5, Plk1 and Tuba6, are presented in Figure 5(B). All these genes were significantly different between WT and Timp1 KO lungs following MWCNT exposure. These results indicate that TIMP1 may affect the MWCNT-induced expression of genes important for cell cycle regulation and thereby promote MWCNT-induced cell proliferation during fibrosis development in the lungs.

We examined the effect of TIMP1 on the proliferation of fibroblasts and myofibroblasts *in vivo*. Double immunofluorescence staining revealed apparent increases in numbers of Hsp47+ and Ki-67+ cells in the fibrotic foci of WT lungs exposed to MWCNTs, in which a portion of the cells were positive for both Hsp47 and Ki-67, indicating the proliferation of fibroblasts within the fibrotic foci (Figure 5C, upper panel). The numbers of Hsp47+ cells and Ki-67+ cells were also increased in MWCNT-exposed Timp1 KO lungs, albeit at

significantly lower levels than WT. Moreover, double-positive fibroblasts for both Hsp47 and Ki-67 were scarce within the fibrotic foci of Timp1 KO lungs. Therefore, loss of TIMP1 significantly reduces fibroblast proliferation in MWCNT-induced fibrosis.

Exposure to MWCNTs increased the number of α-SMA+ myofibroblasts in the fibrotic foci (Figure 5C, lower panel; also Figures 3C, 3D and S8). However, most α-SMA+ myofibroblasts were negative for Ki-67 in both WT and Timp1 KO lungs exposed to MWCNTs (Figure 5C, lower panel). These results suggest that TIMP1 promotes the proliferation of fibroblasts, but not myofibroblasts, in the lungs.

To further corroborate the proliferative effect of TIMP1 on fibroblasts, we tested if an inhibition of TIMP1 by its neutralizing antibodies would mimic the Timp1 KO effect to block or reduce the proliferation of fibroblasts observed in the presence of functional TIMP1 and MWCNTs. Cultured primary lung fibroblasts derived from adult WT mice showed a basal level of proliferation, as demonstrated by a low percentage of the nuclei stained positive for Ki-67 in the presence of DM under the experimental condition (Figure S12). Treatment with TIMP1 neutralizing antibodies did not change the proliferation level. MWCNTs at 5 μg/ml stimulated fibroblast proliferation as expected, with an apparently increased percentage of Ki-67+ cells (from ~15 to ~65%). However, a co-treatment of the cells with MWCNTs and the TIMP1 neutralizing antibodies reduced the level of Ki-67+ cells markedly in comparison with the treatment with MWCNTs alone (from ~65 to ~25%). Therefore, the inhibition of TIMP1 by its neutralizing antibodies effectively reduced TIMP1's proliferative effect on fibroblasts *in vitro*, further supporting the pronounced pro-proliferative activity of TIMP1 on lung fibroblasts.

TIMP1-dependent induction and activation of the TIMP1/CD63/integrin β1 axis and ERK signaling in lung fibroblasts in vivo

TIMP1 may stimulate cellular functions by forming a complex with the cell surface proteins CD63 and integrin β1 that in turn modulates intracellular signaling. Triple immunofluorescence of TIMP1, CD63 and Hsp47 on lung tissue sections showed that there were significant increases in both the fluorescence intensity and the number of positively stained cells in the fibrotic foci of MWCNT-exposed WT lungs compared with DM controls and Timp1 KO lungs (Figure 6A). These increases could be due to the induction of cellular proteins and/or recruitment/proliferation of positively stained cells by MWCNTs in a TIMP1-dependent manner. Notably, more than 80% of the TIMP1 and CD63 fluorescence signals were co-localized on Hsp47+ fibroblasts in MWCNT-treated WT lungs, but not in DM-treated WT, DM-treated Timp1 KO or MWCNT-treated Timp1 KO lungs (Figures 6A and S13A). These results suggest that secreted TIMP1 binds to CD63 on the surface of Hsp47+ fibroblasts in WT lungs exposed to MWCNTs.

The induction of TIMP1 and, to a much lesser extent, CD63 was also observed in a portion of α-SMA+ myofibroblasts in fibrotic foci of WT lungs exposed to MWCNTs (Figure 6B). Although CD63 fluorescence co-localized with TIMP1 and/or α-SMA fluorescence, both the fluorescence intensity and the number of triple-positive cells were significantly lower in myofibroblasts than in fibroblasts (compare Figure 6B with 6A; exemplary myofibroblasts negative for triple co-localization are marked by arrows). The results indicate that there were

reduced expression of CD63 and reduced interaction between TIMP1 and CD63 in α-SMA+ myofibroblasts compared with fibroblasts, which is in agreement with the observation that MWCNTs and TIMP1 affect the proliferation of fibroblasts but not myofibroblasts (Figure 5C).

We examined the co-localization of TIMP1 and integrin β1 in fibroblasts. Triple immunofluorescence of TIMP1, integrin β1 and Hsp47 on lung sections revealed a significantly increased number of cells expressing high levels of integrin β1, as indicated by strong fluorescence staining in WT lungs exposed to MWCNTs (Figure 6C). Furthermore, more than 80% of integrin β1 fluorescence co-localized with TIMP1 and Hsp47 fluorescence, indicating that TIMP1 interacts with the membrane protein integrin β1 on the surface of Hsp47+ fibroblasts in MWCNT-exposed WT lungs (Figures 6C and S13B).

To further verify the co-localization among TIMP1, CD63 and integrin β1 on the cell surface of fibroblasts, we performed triple immunofluorescence staining with cultured primary mouse lung fibroblasts (Figure S14). All three proteins were detected at low levels and co-localized on the cell surface in DM-treated fibroblasts. MWCNTs markedly increased the levels of these proteins, which co-localized most apparently on the cell surface. Thus, both *in vivo* and *in vitro* data support the notion that secreted TIMP1 forms a complex with cell surface proteins CD63 and integrin β1 on fibroblasts in mouse lungs, which is drastically increased by MWCNTs.

The formation of a TIMP1/CD63/integrin β1 complex on the cell surface may lead to activation of the Erk1/2 pathway, which boosts cell proliferation. To test this notion, the induction of phosphorylated Erk1/2, which signifies the activation of ERK signaling, was examined in fibroblasts *in vivo*. Triple immunofluorescence staining of TIMP1, p-Erk1/2 and Hsp47 revealed that exposure to MWCNTs markedly increased the fluorescence intensity of p-Erk1/2, as well as the number of cells positive for p-Erk1/2, to the levels similar to those of TIMP1 and Hsp47 in WT lungs (Figures 6D and S13C). Importantly, a majority of p-Erk1/2+ cells were TIMP1 and Hsp47 double-positive, demonstrating that MWCNTs induce the activation of the ERK pathway in fibroblasts in a TIMP1-dependent manner.

Discussion

Pulmonary exposure to certain forms of MWCNTs induces lung fibrosis in experimental animals that exhibits a high similarity to human lung fibrosing disorders of both induced and idiopathic origins, thus serving as a useful animal model for studying lung fibrosis (Dong et al., 2015). Here, we identified TIMP1 as a highly induced mediator of MWCNT-induced lung fibrosis. Our findings provide new molecular insights into the mechanisms underlying lung fibrosis, and raise the possibility of using TIMP1 as a biomarker for monitoring fibrogenic exposure and fibrosis development, and exploring the TIMP1 signaling pathways for therapeutic development against lung fibrosis.

We first demonstrated marked elevation of TIMP1 expression and secretion in the lungs, BAL and serum by MWCNTs in a time-and dose-dependent manner. Induction was rapid

with the most dramatic increase on day 1 post-exposure (Figure 1). This result extends our previous finding in which Timp1 was shown to be induced in mouse lungs exposed to MWCNTs through a fibrosis-specific PCR array analysis (Dong & Ma, 2016c). We further showed that fibroblasts are a major source of TIMP1 in fibrotic regions, followed by macrophages, on day 7 post-exposure to MWCNTs (Figure S1). Others have reported increased Timp1 mRNA levels in mouse lungs on day 56 and in rat lungs on day 7 and day 30 post-exposure to MWCNTs (van Berlo et al., 2014; Wang et al., 2013). Increased TIMP1 levels were also observed in other lung fibrosis models, such as bleomycin-induced lung fibrosis, and in human lung fibrotic diseases, such as IPF. Therefore, induction of TIMP1 appears to represent a common molecular response in fibrosis and play an important role in fibrosis development, especially during the initiation of inflammation and fibrosing tissue remodeling.

Timp1 KO mice were used to analyze the functional impact of TIMP1 on MWCNT-induced fibrosis in the lungs. Compared with WT, Timp1 KO mice displayed reduced lung fibrosis, as shown by significantly attenuated fibrotic focus formation, ECM deposition, and fibrosis marker protein expression, demonstrating that TIMP1 indeed plays an important role in the development of induced lung fibrosis (Figures 2 and S3–S6). Because fibroblasts and myofibroblasts are the major effector cells in lung fibrosis, we further examined the effects of Timp1 deficiency on these two types of cells in MWCNT-exposed lungs using Hsp47, Vimentin and FSP1 as markers for fibroblasts and α-SMA and PDGFR-β for myofibroblasts. Dramatically increased numbers of fibroblasts and myofibroblasts were detected in MWCNT-treated WT lungs, but this effect was significantly reduced in Timp1 KO lungs (Figures 3, S7 and S8). This finding reveals that MWCNTs increase the numbers of fibroblasts and myofibroblasts in the lungs in a TIMP1-dependent manner.

Increased cellularity is a predominant phenotype in MWCNT-exposed lungs, which presumably arises from inflammatory infiltration, the migration of resident cells or the proliferation of localized cells. By examining the number of cells that were positive for Ki-67 or PCNA, we found that MWCNTs potently stimulated cell proliferation in WT lungs, but the proliferative effect was significantly reduced in Timp1 KO lungs (Figures 4 and S9–S11). Moreover, MWCNTs induced the expression of a panel of cell cycle control genes in WT lungs, but induction was significantly reduced in Timp1 KO lungs (Figure 5A and B); MWCNTs stimulated the proliferation of fibroblasts in WT lungs but not in Timp1 KO lungs (Figure 5C); and co-treatment of primary mouse lung fibroblasts with MWCNTs and TIMP1 neutralizing antibodies largely reduced the proliferation of fibroblasts induced by MWCNTs *in vitro* (Figure S12). Other studies have also suggested a role for TIMP1 in boosting cell proliferation in several *in vitro* and *in vivo* models (Bertaux et al., 1991; Chesler et al., 1995; Friedmann-Morvinski et al., 2016; Hayakawa et al., 1992; Xia et al., 2012). Therefore, our results describe a novel underlying mechanism for MWCNT-induced lung fibrosis through the TIMP1-dependent proliferation of fibroblasts. Importantly, most α-SMA+ myofibroblasts did not co-stain with Ki-67 or PCNA, indicating they were not actively proliferating in MWCNT-exposed lungs. As myofibroblasts derive from fibroblasts through differentiation, this finding suggests that MWCNTs increase the myofibroblast population by promoting their differentiation from fibroblasts but not the proliferation of myofibroblasts themselves. Alternatively, MWCNTs may reduce the turnover of myofibroblasts by

stimulating myofibroblasts to become apoptosis-resistant in a TIMP1-dependent manner during fibrosis development.

The mechanism by which TIMP1 promotes cell proliferation in lung fibrosis is unknown. TIMP1 is a member of the TIMP family of proteins that is traditionally defined as endogenous inhibitors of MMPs. Recent studies have shown that the activity and function of TIMP1 can be mediated through either an MMP-dependent or MMP-independent mechanism (Stetler-Stevenson, 2008). The role of MMP inhibition by TIMP1 in fibrosis development has been controversial, with inconsistent conclusions from different studies, which is partly due to the complex nature of MMPs and their functions. For instance, MMPs have both inhibitory and stimulatory activities toward fibrosis in addition to ECM degradation (Giannandrea & Parks, 2014). On the other hand, the MMP-independent functions of TIMP1, such as promoting cell proliferation and survival, have received increasing attention, particularly for cancer cells (Friedmann-Morvinski et al., 2016; Xia et al., 2012). In this regard, our study provides the *in vivo* evidence to support the MMP-independent function of TIMP1 in promoting cell proliferation in induced organ fibrosis.

In vitro studies have shown that TIMP1 interacts with cell surface CD63 and subsequently associates with integrin β1 in a CD63-dependent manner, forming a supramolecular complex to modulate intracellular signaling (Jung et al., 2006; Toricelli et al., 2013). In a mouse lung cancer model, TIMP1 was identified as a key mediator of tumor growth through its pro-proliferative activity involving high level ERK activation (Xia et al., 2012). TIMP1 was also up-regulated and played a role in tumor proliferation and growth in a mouse glioblastoma multiforme model (Friedmann-Morvinski et al., 2016). These findings prompted us to examine whether TIMP1 stimulates fibroblast proliferation in the lungs exposed to MWCNTs by interacting with CD63, integrin β1 and the ERK pathway. Triple immunofluorescence staining clearly revealed co-localization of TIMP1 and CD63 and co-localization of TIMP1 and integrin β1 in Hsp47+ fibroblasts in MWCNT-exposed lungs (Figures 6A, 6C, S13A and S13B). Furthermore, MWCNT-induced co-localization of TIMP1 with CD63 and integrin β1 was shown to take place in cultured primary mouse lung fibroblasts (Figure S14). These data indicate that MWCNTs significantly induce the expression of CD63 and integrin β1 in addition to TIMP1, and secreted TIMP1 interacts with CD63 and integrin β1 on the cell surface of fibroblasts to regulate intracellular signaling. These findings provide a plausible molecular mechanism to account for the TIMP1-dependent proliferation of fibroblasts for MWCNT-induced fibrosis in the lungs.

The ERK pathway plays multiple roles in physiology and disease, such as modulating cell proliferation. MWCNTs have been shown to stimulate ERK signaling activation in several *in vitro* systems (Ding et al., 2005; Hirano et al., 2010; Lee et al., 2012). However, no *in vivo* study on the effect of MWCNTs on ERK activation has been reported. In this study, we clearly demonstrated that the ERK pathway was remarkably activated in TIMP1 and Hsp47 double-positive fibroblasts in MWCNT-exposed lungs (Figures 6D and S13C). Therefore, MWCNTs induce the activation of the ERK pathway in fibroblasts in the lungs to boost fibroblast proliferation in MWCNT-induced lung fibrosis *in vivo*, which requires the normal function of TIMP1.

Timp1 expression can be up-regulated by activation of the transcription factor nuclear factor-κB (NF-κB) (Wilczynska et al., 2006; Xia et al., 2012). MWCNTs have been shown to activate the NF-κB signaling pathway in macrophages *in vitro*, which potentially contributes to a number of CNT-induced effects including oxidative and apoptotic outcomes (He et al., 2011; Raghu et al., 2011). MWCNTs also induced the time-dependent phosphorylation of NF-κB inhibitor α (IκBα) in cultured rat lung epithelial cells (Ravichandran et al., 2010). We have found that NF-κB is remarkably activated in MWCNT-exposed mouse lungs *in vivo* (Dong & Ma, unpublished data). Therefore, the activation of NF-κB by MWCNTs represents a potential mechanism underlying the pulmonary induction of TIMP1.

In conclusion, we have identified an important function of TIMP1 in the development of MWCNT-induced mouse lung fibrosis that involves TIMP1-stimulated fibroblast proliferation via the interaction of TIMP1/CD63/integrin β1 on the cell surface and the activation of intracellular ERK pathway. Therefore, we provide new evidence for the function of TIMP1 in lung fibrosis, which suggests a new, potential therapeutic target for human fibrotic lung diseases.

Supplementary Material

Refer to Web version on PubMed Central for supplementary material.

Acknowledgments

This work was funded to Q. M. by National Institute for Occupational Safety and Health, Health Effects Laboratory Division and the Nanotechnology Research Center. The findings and conclusions in this report are those of the authors and do not necessarily represent the views of the National Institute for Occupational Safety and Health.

References

Aiso S, Yamazaki K, Umeda Y, Asakura M, Kasai T, Takaya M, et al. Pulmonary toxicity of intratracheally instilled multiwall carbon nanotubes in male Fischer 344 rats. Ind Health. 2010; 48:783–95. [PubMed: 20616469]

Bertaux B, Hornebeck W, Eisen AZ, Dubertret L. Growth stimulation of human keratinocytes by tissue inhibitor of metalloproteinases. J Invest Dermatol. 1991; 97:679–85. [PubMed: 1940438]

Chesler L, Golde DW, Bersch N, Johnson MD. Metalloproteinase inhibition and erythroid potentiation are independent activities of tissue inhibitor of metalloproteinases-1. Blood. 1995; 86:4506–15. [PubMed: 8541540]

De Volder MF, Tawfick SH, Baughman RH, Hart AJ. Carbon nanotubes: present and future commercial applications. Science. 2013; 339:535–9. [PubMed: 23372006]

Ding L, Stilwell J, Zhang T, Elboudwarej O, Jiang H, Selegue JP, et al. Molecular characterization of the cytotoxic mechanism of multiwall carbon nanotubes and nano-onions on human skin fibroblast. Nano Lett. 2005; 5:2448–64. [PubMed: 16351195]

Donaldson K, Murphy FA, Duffin R, Poland CA. Asbestos, carbon nanotubes and the pleural mesothelium: a review of the hypothesis regarding the role of long fibre retention in the parietal pleura, inflammation and mesothelioma. Part Fibre Toxicol. 2010; 7:5. [PubMed: 20307263]

Dong J, Ma Q. Advances in mechanisms and signaling pathways of carbon nanotube toxicity. Nanotoxicology. 2015; 9:658–76. [PubMed: 25676622]

Dong J, Ma Q. *In vivo* activation of a T helper 2-driven innate immune response in lung fibrosis induced by multi-walled carbon nanotubes. Arch Toxicol. 2016a; 90:2231–48. [PubMed: 27106021]

Dong J, Ma Q. Myofibroblasts and lung fibrosis induced by carbon nanotube exposure. Part Fibre Toxicol. 2016b; 13:60. [PubMed: 27814727]

Dong J, Ma Q. Suppression of basal and carbon nanotube-induced oxidative stress, inflammation and fibrosis in mouse lungs by Nrf2. Nanotoxicology. 2016c; 10:699–709. [PubMed: 26592091]

Dong J, Porter DW, Batteli LA, Wolfarth MG, Richardson DL, Ma Q. Pathologic and molecular profiling of rapid-onset fibrosis and inflammation induced by multi-walled carbon nanotubes. Arch Toxicol. 2015; 89:621–33. [PubMed: 25510677]

Dong J, Yu X, Porter DW, Battelli LA, Kashon ML, Ma Q. Common and distinct mechanisms of induced pulmonary fibrosis by particulate and soluble chemical fibrogenic agents. Arch Toxicol. 2016; 90:385–402. [PubMed: 26345256]

Friedmann-Morvinski D, Narasimamurthy R, Xia Y, Myskiw C, Soda Y, Verma IM. Targeting NF-κB in glioblastoma: a therapeutic approach. Sci Adv. 2016; 2:e1501292. [PubMed: 26824076]

Giannandrea M, Parks WC. Diverse functions of matrix metal-loproteinases during fibrosis. Dis Model Mech. 2014; 7:193–203. [PubMed: 24713275]

Hayakawa T, Yamashita K, Tanzawa K, Uchijima E, Iwata K. Growth-promoting activity of tissue inhibitor of metalloproteinases-1 (TIMP-1) for a wide range of cells. A possible new growth factor in serum. FEBS Lett. 1992; 298:29–32. [PubMed: 1544418]

Hayashi T, Stetler-Stevenson WG, Fleming MV, Fishback N, Koss MN, Liotta LA, et al. Immunohistochemical study of metalloproteinases and their tissue inhibitors in the lungs of patients with diffuse alveolar damage and idiopathic pulmonary fibrosis. Am J Pathol. 1996; 149:1241–56. [PubMed: 8863673]

He X, Young SH, Schwegler-Berry D, Chisholm WP, Fernback JE, Ma Q. Multiwalled carbon nanotubes induce a fibrogenic response by stimulating reactive oxygen species production, activating NF-κB signaling, and promoting fibroblast-to-myofibroblast transformation. Chem Res Toxicol. 2011; 24:2237–48. [PubMed: 22081859]

Hinz B. The myofibroblast: paradigm for a mechanically active cell. J Biomech. 2010; 43:146–55. [PubMed: 19800625]

Hirano S, Fujitani Y, Furuyama A, Kanno S. Uptake and cytotoxic effects of multi-walled carbon nanotubes in human bronchial epithelial cells. Toxicol Appl Pharmacol. 2010; 249:8–15. [PubMed: 20800606]

Johnston HJ, Hutchison GR, Christensen FM, Peters S, Hankin S, Aschberger K, et al. A critical review of the biological mechanisms underlying the *in vivo* and *in vitro* toxicity of carbon nanotubes: the contribution of physico-chemical characteristics. Nanotoxicology. 2010; 4:207–46. [PubMed: 20795897]

Jung KK, Liu XW, Chirco R, Fridman R, Kim HR. Identification of CD63 as a tissue inhibitor of metalloproteinase-1 interacting cell surface protein. EMBO J. 2006; 25:3934–42. [PubMed: 16917503]

Lee JK, Sayers BC, Chun KS, Lao HC, Shipley-Phillips JK, Bonner JC, et al. Multi-walled carbon nanotubes induce COX-2 and iNOS expression via MAP kinase-dependent and -independent mechanisms in mouse RAW264.7 macrophages. Part Fibre Toxicol. 2012; 9:14. [PubMed: 22571318]

Madtes DK, Elston AL, Kaback LA, Clark JG. Selective induction of tissue inhibitor of metalloproteinase-1 in bleomycin-induced pulmonary fibrosis. Am J Respir Cell Mol Biol. 2001; 24:599–607. [PubMed: 11350830]

Manoury B, Caulet-Maugendre S, Guenon I, Lagente V, Boichot E. TIMP-1 is a key factor of fibrogenic response to bleomycin in mouse lung. Int J Immunopathol Pharmacol. 2006; 19:471–87. [PubMed: 17026855]

Porter DW, Hubbs AF, Mercer RR, Wu N, Wolfarth MG, Sriram K, et al. Mouse pulmonary dose- and time course-responses induced by exposure to multi-walled carbon nanotubes. Toxicology. 2010; 269:136–47. [PubMed: 19857541]

Raghu G, Collard HR, Egan JJ, Martinez FJ, Behr J, Brown KK, et al. An official ATS/ERS/JRS/ALAT statement: idiopathic pulmonary fibrosis: evidence-based guidelines for diagnosis and management. Am J Respir Crit Care Med. 2011; 183:788–824. [PubMed: 21471066]

Ravichandran P, Baluchamy S, Sadanandan B, Gopikrishnan R, Biradar S, Ramesh V, et al. Multiwalled carbon nanotubes activate NF-κB and AP-1 signaling pathways to induce apoptosis in rat lung epithelial cells. Apoptosis. 2010; 15:1507–16. [PubMed: 20694747]

Reddy AR, Reddy YN, Krishna DR, Himabindu V. Pulmonary toxicity assessment of multiwalled carbon nanotubes in rats following intratracheal instillation. Environ Toxicol. 2012; 27:211–19. [PubMed: 20862737]

Selman M, Ruiz V, Cabrera S, Segura L, Ramirez R, Barrios R, et al. TIMP-1, −2, −3, and −4 in idiopathic pulmonary fibrosis. A prevailing nondegradative lung microenvironment? Am J Physiol Lung Cell Mol Physiol. 2000; 279:L562–74. [PubMed: 10956632]

Stetler-Stevenson WG. Tissue inhibitors of metalloproteinases in cell signaling: metalloproteinase-independent biological activities. Sci Signal. 2008; 1:re6. [PubMed: 18612141]

Tomasek JJ, Gabbiani G, Hinz B, Chaponnier C, Brown RA. Myofibroblasts and mechano-regulation of connective tissue remodelling. Nat Rev Mol Cell Biol. 2002; 3:349–63. [PubMed: 11988769]

Tomita M, Okuyama T, Katsuyama H, Miura Y, Nishimura Y, Hidaka K, et al. Mouse model of paraquat-poisoned lungs and its gene expression profile. Toxicology. 2007; 231:200–9. [PubMed: 17215068]

Toricelli M, Melo FH, Peres GB, Silva DC, Jasiulionis MG. TIMP1 interacts with beta-1 integrin and CD63 along melanoma genesis and confers anoikis resistance by activating PI3-K signaling pathway independently of Akt phosphorylation. Mol Cancer. 2013; 12:22. [PubMed: 23522389]

van Berlo D, Wilhelmi V, Boots AW, Hullmann M, Kuhlbusch TA, Bast A, et al. Apoptotic, inflammatory, and fibrogenic effects of two different types of multi-walled carbon nanotubes in mouse lung. Arch Toxicol. 2014; 88:1725–37. [PubMed: 24664304]

Wang P, Nie X, Wang Y, Li Y, Ge C, Zhang L, et al. Multiwall carbon nanotubes mediate macrophage activation and promote pulmonary fibrosis through TGF-β/Smad signaling pathway. Small. 2013; 9:3799–811. [PubMed: 23650105]

Wilczynska KM, Gopalan SM, Bugno M, Kasza A, Konik BS, Bryan L, et al. A novel mechanism of tissue inhibitor of metalloproteinases-1 activation by interleukin-1 in primary human astrocytes. J Biol Chem. 2006; 281:34955–64. [PubMed: 17012236]

Wynn TA, Ramalingam TR. Mechanisms of fibrosis: therapeutic translation for fibrotic disease. Nat Med. 2012; 18:1028–40. [PubMed: 22772564]

Xia Y, Yeddula N, Leblanc M, Ke E, Zhang Y, Oldfield E, et al. Reduced cell proliferation by IKK2 depletion in a mouse lung-cancer model. Nat Cell Biol. 2012; 14:257–65. [PubMed: 22327365]

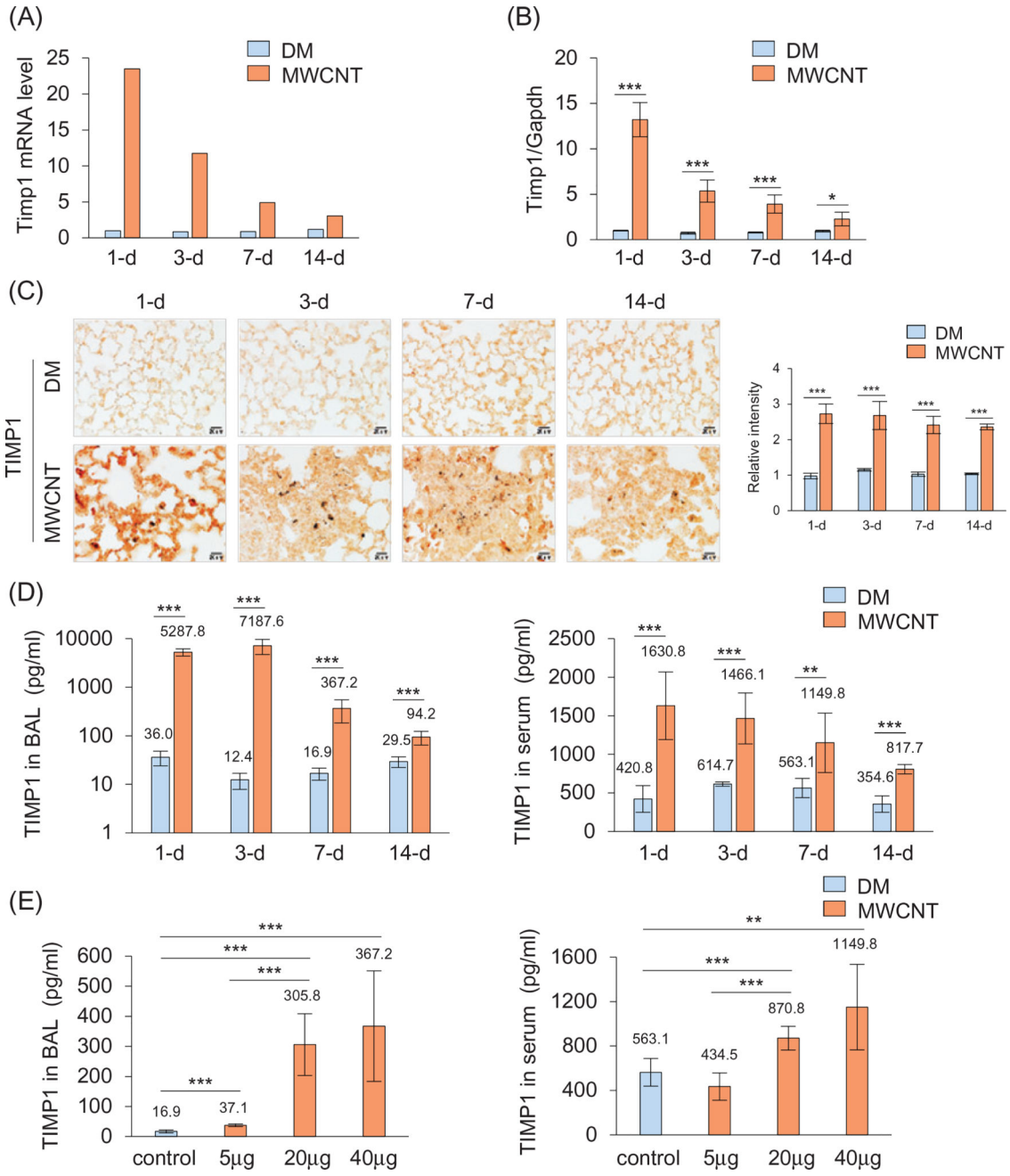

Figure 1.

Induction of Timp1 by MWCNTs. WT mice received DM or MWCNTs (40 μg) and were sacrificed on days 1, 3, 7, and 14 post-exposure (A–D). (A) Mouse fibrosis PCR array. Pooled lung tissue total RNA from six mice each group was analyzed. Fold changes are presented. (B) qRT-PCR analysis ($n = 4$). (C) Immunohistochemistry of TIMP1 (red, scale bar: 20 μm). The relative intensity of positive staining is presented as the mean ± SD ($n = 4$) on the right. (D) TIMP1 protein levels in the BAL fluid and serum detected by ELISA (mean ± SD, $n = 5–6$). (E) Dose dependence. WT mice were treated with DM or MWCNTs (5, 20

or 40 μg) for 7 d. TIMP1 protein levels in the BAL fluid and serum were determined by ELISA (mean ± SD, n = 5–6).

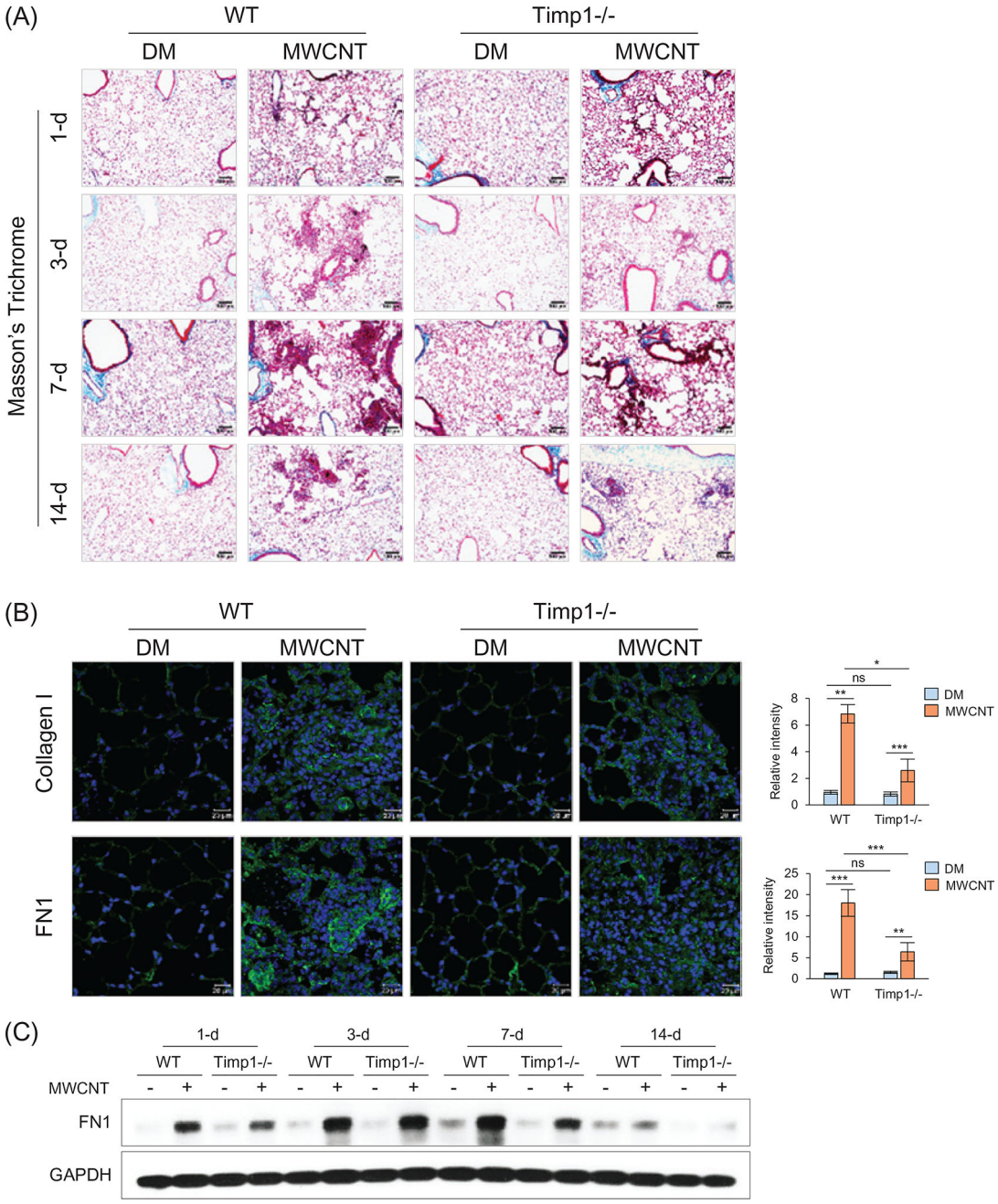

Figure 2.

Reduced fibrosis in Timp1 KO lungs. WT and Timp1 KO mice received DM or MWCNTs (40 μg). (A) Masson's Trichrome staining. Time course is shown. Scale bar: 100 μm. (B) Collagen I (upper panel) and FN1 (lower panel) immunofluorescence staining (green indicates positive staining, blue represents nuclear staining) on lung sections from mice sacrificed on day 7 post-exposure. Scale bar: 20 μm. Relative intensity is shown as the mean ± SD (n = 4). (C) Immunoblotting of FN1. Lung proteins from randomly selected samples of each group were analyzed and a representative blotting image is presented.

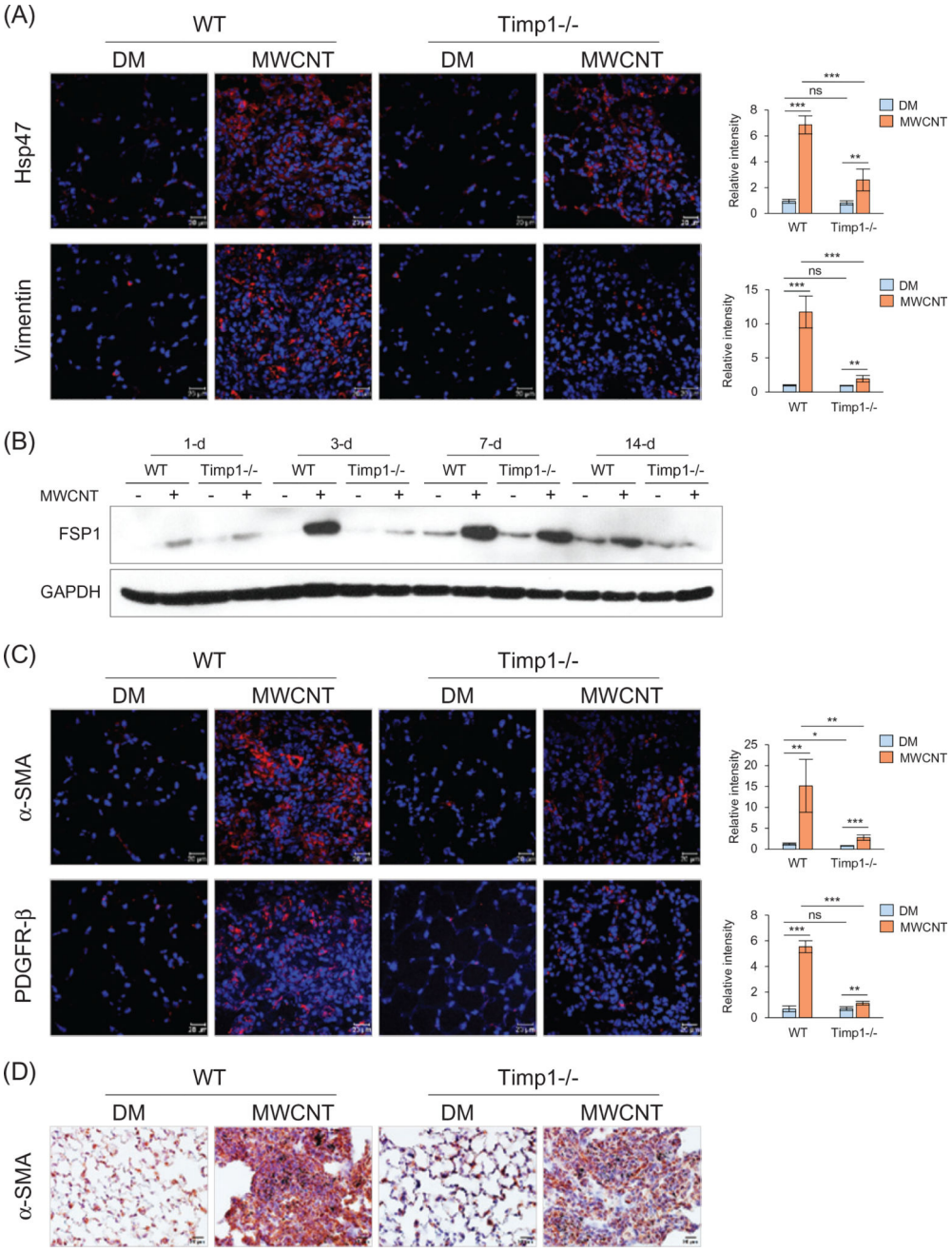

Figure 3.

Recruitment of fibroblasts and myofibroblasts by MWCNTs. Lung sections from mice exposed to DM or 40 μg MWCNTs for 7 d were examined for the expression of fibroblast and myofibroblast markers (A, C and D). (A) Immunofluorescence detection of fibroblast markers Hsp47 and Vimentin. (B) Immunoblotting of FSP1. Lung proteins from randomly selected samples of each group exposed to DM or 40 μg MWCNTs were analyzed and a representative blotting image is presented. (C) Immunofluorescence detection of myofibroblast markers α-SMA and PDGFR-β. (D) Immunohistochemistry staining of α-SMA. Images have scale bars of 20 μm. For (A) and (C), the red color indicates positive

staining and blue indicates nuclear staining. Relative intensity is shown as the mean ± SD (n = 4).

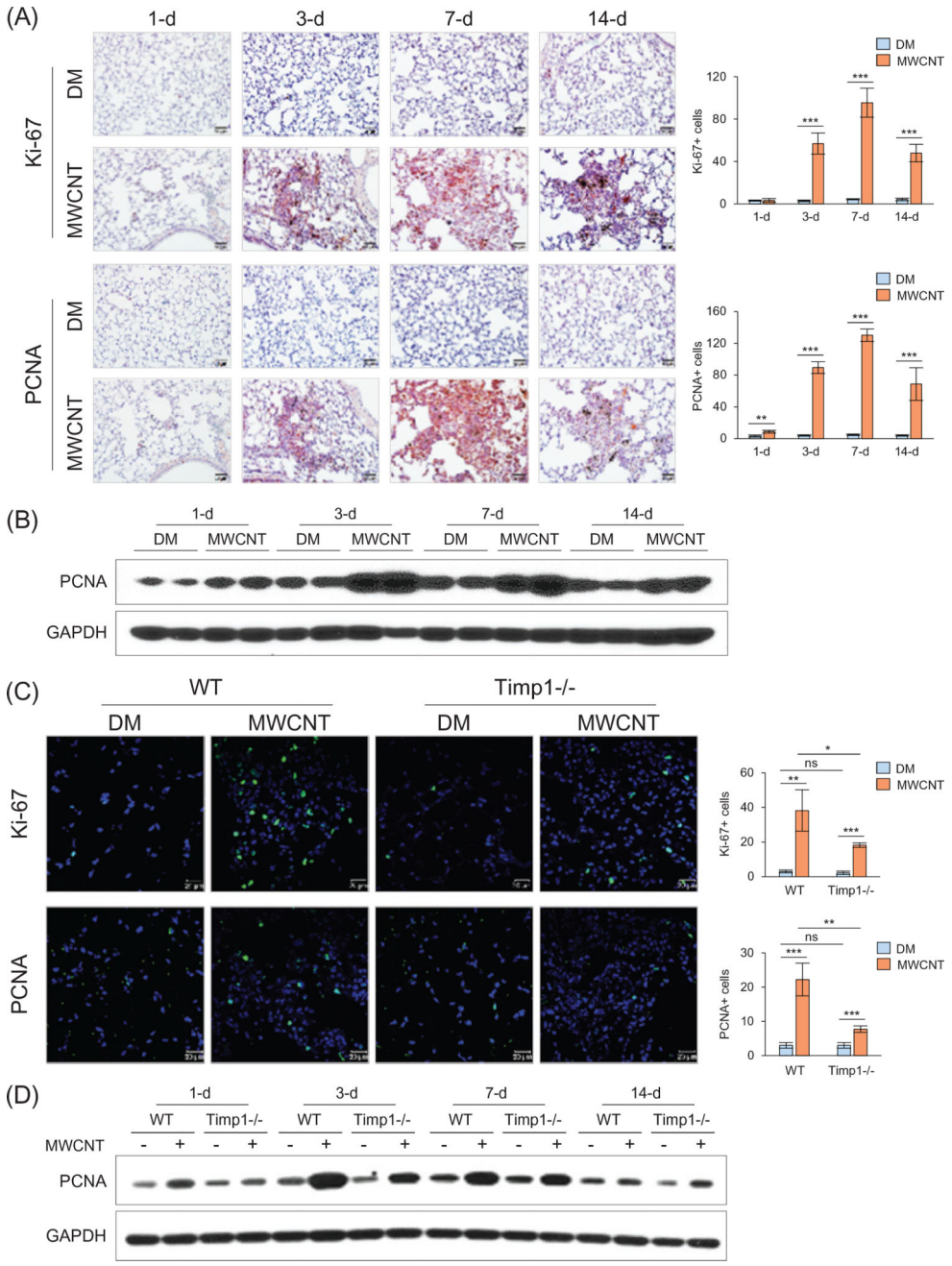

Figure 4.

Reduced cell proliferation in Timp1 KO lungs. (A and B) Time-dependent stimulation of cell proliferation by MWCNTs (40 μg) in WT lungs on days 1, 3, 7 and 14 post-exposure. (A) Immunohistochemistry of Ki-67 (upper panel) and PCNA (lower panel) on lung sections of WT mice. Red indicates positive staining and blue nuclear counterstaining. Scale bar: 20 μm. The number of cells with positive staining is shown as the mean ± SD ($n = 4$). (B) Immunoblotting of PCNA in lung tissues of WT mice. Lung proteins from two randomly selected samples of each group were used. (C and D) Comparison of cell proliferation between WT and Timp1 KO lungs exposed to MWCNTs (40 μg). (C) Immunofluorescence

of Ki-67 (upper panel) and PCNA (lower panel) on lung sections (7 d post-exposure). Green indicates positive staining and blue nuclear staining. Scale bar: 20 μm. The number of cells with positive staining is shown as the mean ± SD (n = 4). (D) Immunoblotting of PCNA. Lung proteins from randomly selected samples of each group were studied, and a representative blotting image is presented.

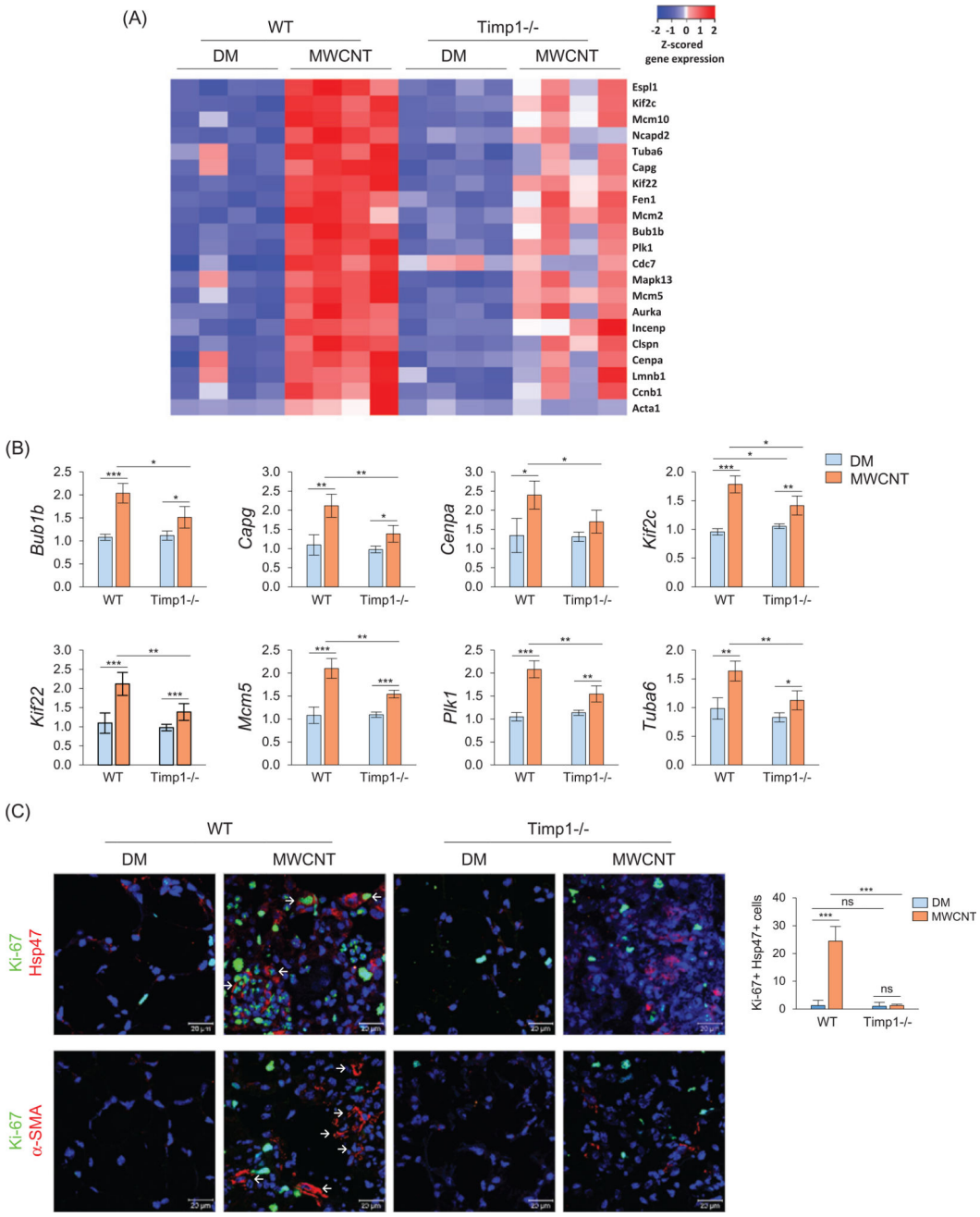

Figure 5.

TIMP1-mediated stimulation of gene expression and fibroblast proliferation by MWCNTs. Mice were exposed to DM or 40 μg MWCNTs for 7 d. (A) Heat map of cell cycle control genes identified by microarray. Total RNA isolated from individual mice was used ($n = 4$, for each genotype and treatment group). Red, white and blue indicate high, medium and low expression levels, respectively. (B) Examples of up-regulated genes shown in the heat map are presented with fold changes and p values ($n = 4$). *$p < 0.05$; ** $p < 0.01$; and ***$p < 0.001$. (C) Cell proliferation. Proliferation of fibroblasts was examined by double immunofluorescence staining of Ki-67 (green) and Hsp47 (red), with double-positive cells

showing green staining in the nucleus and red staining outside of the nucleus (upper panel, scale bar: 20 μm, example cells are indicated by arrows). The number of Ki-67 and Hsp47 double-positive cells is shown as the mean ± SD (n = 4). Proliferation of myofibroblasts was examined by double immunofluorescence staining of Ki-67 (green) and α-SMA (red) (lower panel, scale bar: 20 μm). Blue indicates nuclear staining. Representative myofibroblasts are indicated by arrows, showing strong staining for α-SMA but weak or no co-staining for Ki-67.

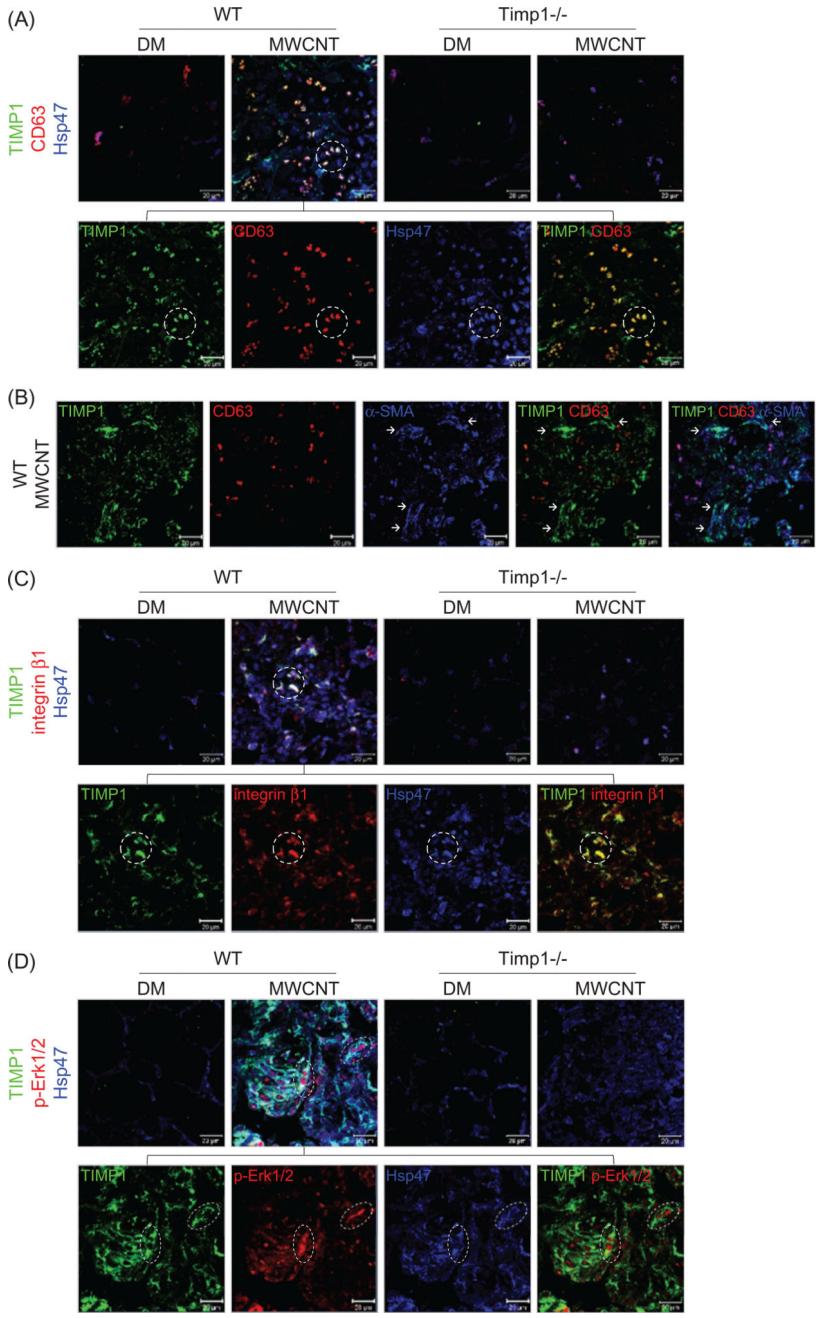

Figure 6.

Induction and co-localization of TIMP1, CD63, and integrin β1 and activation of ERK. Mice were exposed to DM or 40 μg MWCNTs for 7 d. (A) Induction and co-localization of TIMP1 and CD63 in fibroblasts detected by triple immunofluorescence of TIMP1 (green), CD63 (red) and Hsp47 (blue) on lung sections. Scale bar: 20 lm. Circled cells illustrate representative triple-positive cells. (B) Induction and co-localization of TIMP1 and CD63 in myofibroblasts examined by triple immunofluorescence of TIMP1 (green), CD63 (red) and α-SMA (blue) on lung sections from MWCNT-exposed WT mice. Images of single staining and merged images of double and triple staining are presented, showing the strong induction

and co-localization of TIMP1 and α-SMA, but markedly reduced induction of CD63 and co-localization of CD63 with TIMP1 in myofibroblasts. A subset of TIMP1+ cells are co-localized with α-SMA+ CD63− cells (indicated by arrows). Scale bar: 20 μm. (C) Induction and co-localization of TIMP1 and integrin β1 in fibroblasts detected by triple immunofluorescence of TIMP1 (green), integrin β1 (red) and Hsp47 (blue) on lung sections. Example triple-positive cells are circled. Scale bar: 20 μm. (D) The level of p-Erk1/2 in fibroblasts examined by triple immunofluorescence of TIMP1 (green), p-Erk1/2 (red) and Hsp47 (blue) on lung sections (scale bar: 20 μm). Example triple-positive cells are indicated in the oval.